

# Human adipose-derived mesenchymal stem cell-conditioned media suppresses inflammatory bone loss in a lipopolysaccharide-induced murine model

YU LI<sup>1</sup>, XIN GAO<sup>2</sup> and JINBING WANG<sup>3,4</sup>

<sup>1</sup>Department of Plastic and Reconstructive Surgery, Shanghai Key Laboratory of Tissue Engineering, Shanghai Ninth People's Hospital, Shanghai Jiao Tong University School of Medicine; <sup>2</sup>Department of Oral Implantology, Shanghai Stomatological Hospital; <sup>3</sup>Department of Oral and Maxillofacial-Head and Neck Oncology, Shanghai Ninth People's Hospital, Shanghai Jiao Tong University School of Medicine; <sup>4</sup>Shanghai Key Laboratory of Stomatology and Shanghai Research Institute of Stomatology, National Clinical Research Center of Stomatology, Shanghai 200011, P.R. China

Received October 17, 2016; Accepted September 29, 2017

DOI: 10.3892/etm.2017.5606

**Abstract.** Conditioned media (CM) from mesenchymal stem cells (MSCs) contains various cytokines, growth factors and microRNAs, which may serve important roles in modulating the inflammatory process. However, the effect of MSC-CM on inflammatory bone loss remains unknown. The present study investigated the effects of conditioned media from human adipose-derived mesenchymal stem cells (AMSC-CM) on the prevention of lipopolysaccharide (LPS)-mediated bone loss in mice. To investigate the underlying mechanisms of this effect, the effects of AMSC-CM on serum levels of inflammation-associated cytokines [tumor necrosis factor (TNF)- $\alpha$ , interleukin (IL)-1, IL-6 and IL-10] in LPS-treated mice, in addition to their mRNA expression in LPS-treated macrophages, was investigated. Micro-computed tomography and histological analysis revealed that AMSC-CM administration effectively inhibited LPS-induced bone destruction *in vivo*. ELISA analysis indicated that AMSC-CM significantly reduced the serum levels of proinflammatory cytokines (TNF- $\alpha$ , IL-1 and IL-6) in LPS-treated mice. Furthermore, AMSC-CM treatment significantly decreased the mRNA expression levels of TNF- $\alpha$ , IL-1 and IL-6 in macrophages treated with LPS. These findings indicate that AMSC-CM inhibits LPS-induced bone loss by decreasing the production of proinflammatory cytokines, suggesting that the use of

AMSC-CM may be a potential therapeutic strategy for the treatment of inflammatory bone loss.

## Introduction

The mineralized structure of bone was considered to be relatively inert for a long time; however, the bone is a dynamic tissue that is constantly remodeled by the synergistic effects of osteoblast-mediated bone formation and osteoclast-induced bone resorption (1). Numerous inflammatory diseases may occur as a result of an imbalance between bone production and resorption, leading to bone loss and the deterioration of bone quality. These inflammatory diseases include periodontitis, rheumatoid arthritis and inflammatory bowel disease (2-4). Patients suffering from inflammatory bone loss typically have an increased risk of morbidity and mortality, which may seriously impair their quality of life and thus cause a heavy economic burden (5,6). Therefore, intervention strategies through which inflammatory bone loss can be mitigated are highly valuable.

Mesenchymal stem cells (MSCs) are multipotent stem cells that have a fibroblast-like morphology and can be isolated from various tissues, including bone marrow, adipose tissue and the umbilical cord (7). The multipotent nature of MSCs allows them to self-renew and differentiate into several mesodermal tissues, including bone, cartilage, fat and muscle. Over the past decades, MSCs have drawn much interest for their therapeutic benefits in immune modulation and tissue remodeling (8-10). However, the clinical use of MSCs remains challenging. The MSCs therapy cannot provide an immediate treatment because of the long waiting time for cell preparation. In addition, the survival time of the implanted cells is short, which greatly impairs the therapeutic effect of MSCs (11,12). Furthermore, certain studies have suggested that the transplantation of MSCs into normal tissues may cause tumor formation (13,14).

A growing number of studies have suggested that the principal beneficial effects of MSCs are likely mediated via paracrine mechanisms rather than replication or

---

*Correspondence to:* Dr Jinbing Wang, Department of Oral and Maxillofacial-Head and Neck Oncology, Shanghai Ninth People's Hospital, Shanghai Jiao Tong University School of Medicine, 639 Zhizaoju Road, Shanghai 200011, P.R. China  
E-mail: drjinbing@126.com

**Key words:** cytokines, inflammation, bone resorption, bone loss, mesenchymal stem cells, conditioned media

differentiation (15-17). Indeed, it has been established that MSCs secrete a broad repertoire of bioactive factors, including cytokines, growth factors, microRNAs, proteasomes and exosomes, which may serve an important role in the inflammatory response (17). The bioactive factors secreted by MSCs can be collected in the conditioned media (CM) during cell culture. Previous studies have revealed that the CM from MSCs (MSC-CM) can modulate immune responses and protect against inflammation-induced tissue lesions (18-21). Furthermore, using MSC-CM is more economical and practical for clinical application, since it overcomes several limitations of using MSCs, including invasive cell collection procedures, potential tumorigenicity and a long waiting time for cell expansion (22). In addition, MSC-CM could be mass-produced by tailor-made cell lines under controlled laboratory conditions, providing a convenient resource of bioactive factors.

In the present study, the potential ameliorative effects of human adipose-derived MSC-CM (AMSC-CM) on the bone loss triggered by inflammation was investigated. Human AMSCs were chosen to prepare CM because their harvesting is technically easy, relatively safe and free of ethical concerns. The experiment was performed *in vivo* and *in vitro*. For the *in vivo* study, the effects of AMSC-CM on bone destruction and the serum levels of inflammation-associated cytokines [tumor necrosis factor (TNF)- $\alpha$ , interleukin (IL)-1, IL-6, and IL-10] were investigated in a mouse model of bone loss induced by lipopolysaccharide (LPS). The present study also included an *in vitro* investigation into the effects of AMSC-CM on the mRNA expression levels of inflammation-associated cytokines in macrophages stimulated by LPS to provide insight into the possible mechanism of the beneficial action.

## Materials and methods

**Isolation and culture of human AMSCs.** Abdominal adipose tissues were harvested from donors who underwent liposuction surgery. All donors provided written informed consent and the present study had approval from the Research Ethics Committee of the Shanghai Ninth People's Hospital (Shanghai, China). Briefly, adipose tissues were washed three times with PBS (Sigma-Aldrich; Merck KGaA, Darmstadt, Germany) containing 1% penicillin-streptomycin (Invitrogen; Thermo Fisher Scientific, Inc., Waltham, MA, USA) and minced using scissors. Subsequently, the minced tissues were digested in 0.075% type I collagenase solution (Sigma-Aldrich; Merck KGaA) and incubated in a shaking water bath at 37°C for 1 h. Following incubation, the tissues were centrifuged at 500 x g for 20 min at 4°C. Then, the supernatant was discarded and the pellet was diluted with Dulbecco's modified Eagle's medium (DMEM; Hyclone; GE Healthcare Life Sciences, Logan, UT, USA) supplemented with 10% fetal bovine serum (FBS; Gibco; Thermo Fisher Scientific, Inc.) and 1% penicillin-streptomycin. The cells were filtered through a 100- $\mu$ m nylon mesh (Nanjing Jiancheng Bioengineering Institute, Nanjing, China) and centrifuged again at 500 x g for 5 min at 4°C. The supernatant was then discarded and the cells were cultured in T75 flasks (BD Biosciences, Franklin Lakes, NJ, USA) at 37°C in a humidified incubator containing 5% CO<sub>2</sub>. A total of 48 h later, the culture media was changed, removing non-adherent

cells. For AMSC expansion, the cells were seeded at a density of 2x10<sup>4</sup> cells/cm<sup>2</sup> in T75 flasks and the culture media was changed twice a week. The AMSCs obtained at the end of the third passage were used for the subsequent experiments.

**Characterization of human AMSCs.** The expression of cluster of differentiation (CD) markers of AMSCs were analyzed by flow cytometry. Briefly, a total of 2x10<sup>5</sup> AMSCs were harvested and suspended in PBS containing 4% FBS. Then, the cells were incubated with fluorescence-conjugated antibodies directed against human CD29 (cat. no. 557332), CD34 (cat. no. 550761), CD44 (cat. no. 562818), CD45 (cat. no. 563792), CD90 (cat. no. 555595) and CD105 (cat. no. 563803) (all from BD Biosciences; 1:20 dilution) for 30 min in the dark at 4°C. After being washed three times with PBS, the stained cells were sorted using a FACSCalibur flow cytometer (BD Biosciences). The result was analyzed using BD FACStation software (version 6.1x, BD Biosciences).

The capability for tri-lineage differentiation (osteocyte, chondrocyte and adipocyte) of the AMSCs was also examined. Osteogenic induction was performed using differentiation media consisting of DMEM supplemented with 10% FBS, 50 mg/ml of ascorbic acid, 10 mM  $\beta$ -glycerophosphate and 100 nM dexamethasone (all Sigma-Aldrich; Merck KGaA). The media was changed every 3 days until day 21. Adipogenic studies were performed by culturing the cells in differentiation media containing 1 mM dexamethasone, 50 mM 3-isobutyl-1-methylxanthine and 10 mg/ml insulin (all Sigma-Aldrich; Merck KGaA). For chondrogenesis, 1x10<sup>5</sup> cells were centrifuged at 500 x g in a polypropylene tube (15 ml; BD Biosciences) for 10 min at 4°C. Aggregates were incubated in chondrogenic media consisting of DMEM supplemented with 10% FBS, 1% insulin-transferrin-selenium, 1 mM sodium pyruvate and 50 mM L-proline (all Sigma-Aldrich; Merck KGaA). After the differentiation processes were complete, cells were in 4% paraformaldehyde for 30 min at 37°C and stained with Alizarin Red (10 min at 37°C), Oil Red O (10 min at 37°C) and Toluidine Blue (30 min at 37°C) (all Beyotime Institute of Biotechnology, Haimen, China), respectively. Following this, the cells were observed with a light microscope (Optiphot; Nikon Corp., Tokyo, Japan) at a high-power magnification of x100.

**Preparation of CM.** When the AMSCs reached 80-90% confluency, they were washed three times with warm PBS and the medium was replaced with serum-free DMEM containing 1% penicillin-streptomycin. The CM were collected after 48 h of culture. Then, the collected CM was filtered through a 0.2- $\mu$ m filter (EMD Millipore, Billerica, MA, USA) and concentrated 50-fold using ultrafiltration with a 3 kDa molecular weight cut-off. The concentrated CM was stored at -80°C until required for use in the following experiments.

**LPS-induced bone loss model and histomorphometric analysis.** Animal experiments were performed with ethical approval from the Animal Care and Use Committee of the Shanghai Ninth People's Hospital. A total of 18 5-week-old male ICR mice with an average weight of 30 $\pm$ 1.2 g were randomly divided into a control group (n=6), an LPS group (n=6) and an LPS+CM group (n=6). LPS (5 mg/kg; Sigma-Aldrich; Merck KGaA) was

intraperitoneally injected into the LPS and LPS+CM group mice on days 1 and 4. CM or PBS (2  $\mu$ l/g) were injected into the tail vein of the LPS+CM or control group mice, respectively, every other day for 8 days. After 8 days, the mice were sacrificed, and their left femurs were excised and fixed in 4% paraformaldehyde for  $\geq$ 48 h at 37°C. The bone tissue was then detected and imaged using micro-computed tomography (CT) (eXplore Locus SP Micro-CT; GE Healthcare, Chicago, IL, USA) with a source voltage of 45 kV, current of 80 mA and resolution of 20  $\mu$ m. Bone loss-associated parameters were analyzed using CTAn software (version 1.13; Bruker Corporation, Ettlingen, Germany). After detection by micro-CT, the samples were decalcified in 10% EDTA (Sigma-Aldrich; Merck KGaA) and subsequently embedded in paraffin. For histologic examination, the surface of each section (7- $\mu$ m-thick) was stained with hematoxylin and eosin (H&E; Beyotime Institute of Biotechnology).

*Cytokine analysis in the peripheral blood.* Commercial ELISA kits for TNF- $\alpha$  (cat. no. HSTA00E), IL-1 (cat. no. MLB00C), IL-6 (cat. no. D6050) and IL-10 (cat. no. M1000B) (all from R&D Systems, Inc., Minneapolis, MN, USA) were used to determine the concentrations of inflammation-associated cytokines in the serum according to manufacturer's protocol.

*RAW264.7 cell culture and treatment.* The mouse macrophage-like cell line RAW264.7 was purchased from the Type Culture Collection of the Chinese Academy of Sciences (Shanghai, China) and cultured in high glucose DMEM (Hyclone; GE Healthcare Life Sciences) supplemented with 10% FBS. The cells were cultured in 6-well plates (BD Biosciences) at a density of  $1 \times 10^5$  cells/well. Once the cells reached 80% confluency, they were divided into control, LPS (1  $\mu$ g/ml LPS), CM-1 (1  $\mu$ g/ml LPS + 10  $\mu$ l/ml CM), CM-2 (1  $\mu$ g/ml LPS + 15  $\mu$ l/ml CM) and CM-3 (1  $\mu$ g/ml LPS + 25  $\mu$ l/ml CM) groups. After 24 h, culture media was removed and total RNA was extracted by adding 0.3-0.4 ml of TRIzol reagent (cat. no. 15596018; Thermo Fisher Scientific, Inc., MA, USA) per  $1 \times 10^5$ - $10^7$  cells directly to culture dish.

*Reverse transcription-quantitative polymerase chain reaction (RT-qPCR) analysis.* Total RNA from the RAW 264.7 cells was reverse transcribed into cDNA using high capacity cDNA reverse transcription kit (cat. no. 4368813; Thermo Fisher Scientific, Inc.) according to the manufacturer's protocol. The thermocycling conditions comprised an initial step at 25°C for 10 min, followed by 120 min at 37°C, and 85°C for 5 min. qPCR was performed using mouse-specific primers for TNF- $\alpha$ , IL-1 $\beta$ , IL-6 and IL-10 (Table I) with SYBR Green Master Mix (cat. no. 309155; Thermo Fisher Scientific, Inc.).  $\beta$ -actin was used as the internal control. The thermocycling conditions for qPCR were as follows: Pre-denaturation at 95°C for 10 min; 30 cycles of amplification with denaturation at 95°C for 15 sec, and annealing and extension at 60°C for 1 min; and a final dissociation cycle at 95°C for 15 sec, 60°C for 1 min and 95°C for 15 sec. The  $2^{-\Delta\Delta C_q}$  method was used to calculate the relative expression level for each gene (23).

*Statistical analysis.* All data are presented as the mean  $\pm$  standard deviation from three independent experiments.

Table I. Primer sequences for quantitative polymerase chain reaction analysis.

Gene	Primer (5'-3')	
	Forward	Reverse
TNF- $\alpha$	AACTCCAGGCGG TGCCTATG	TCCAGCTGCTCCT CCACTTG
IL-1	AGCTTCAGGCAG GCAGTATC	TCATCTCGGAGCC TGTAGTG
IL-6	AAGTCCGGAGAG GAGACTTC	TGGATGGTCTTGG TCCTTAG
IL-10	ACTCTTCACCTGC TCCACTG	GCTATGCTGCCTGC TCTTAC
$\beta$ -actin	CACGAACTACCT TCAACTCC	CATACTCCTGCTTG CTGATC

TNF, tumor necrosis factor; IL, interleukin.

The results were statistically evaluated by one-way analysis of variance with a post hoc Tukey's range test using SPSS software (version 15.0; SPSS, Inc., Chicago, IL, USA).  $P < 0.05$  was considered to indicate a statistically significant difference.

## Results

*Characterization of AMSCs.* Passage 3 AMSCs were analyzed for surface antigen expression using flow cytometry. The cells were positive for MSC markers (CD29, CD90 and CD105), but negative for the endothelial cell marker CD31 and the hematopoietic cell marker CD45 (Fig. 1A). In addition, the tri-lineage differentiation capacity of the AMSCs was confirmed through *in vitro* osteogenic (Fig. 1B), adipogenic (Fig. 1C) and chondrogenic (Fig. 1D) induction assays. The cells exhibited the typical characteristics of MSCs and were used in the following experiments.

*AMSC-CM reduces LPS-induced bone loss in vivo.* A mouse model of endotoxin-induced bone loss was used to examine the therapeutic effects of AMSC-CM on inflammatory osteoporosis *in vivo*. In order to improve the therapeutic effect, AMSC-CM was concentrated 50 times by ultrafiltration. Mice were injected with LPS intraperitoneally and then treated with AMSC-CM or PBS. After 8 days of treatment, the mice were sacrificed. Micro-CT revealed that LPS injection led to marked trabecular bone loss in the femurs, but that administration of AMSC-CM visibly inhibited this LPS-induced bone destruction (Fig. 2A). To explore the effect of AMSC-CM on bone erosion more precisely, the three-dimensional reconstruction results of the trabecular bone in the distal femurs were further analyzed (Fig. 2B and C). The bone mineral density (BMD) of the LPS group was significantly lower compared with that of the control group, and the LPS+CM group showed a significant increase in BMD compared with the LPS group. The LPS-induced decrease in bone volume per tissue volume (BV/TV) was also significantly attenuated by AMSC-CM. Consistent with the measurement results of BMD and BV/TV, the trabecular number (Tb.N) of

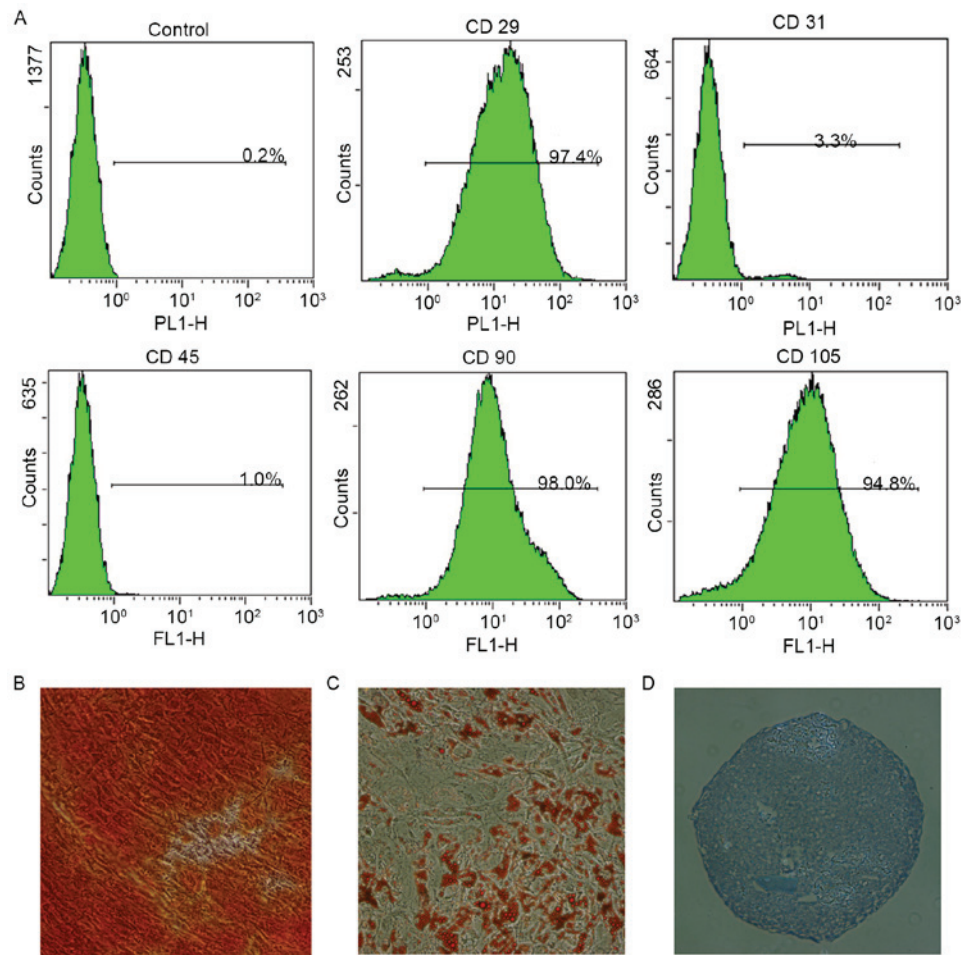


Figure 1. Identification of stem cell markers and the multipotency of human AMSCs. (A) Flow cytometric analyses demonstrated that AMSCs in passage 3 were positive for CD29, CD90 and CD105, but negative for CD31 and CD45. The (B) osteogenic, (C) adipogenic and (D) chondrogenic differentiation of AMSCs was confirmed by Alizarin Red S, Oil Red O and Toluidine Blue staining, respectively. Magnification, x100. AMSC, adipose-derived mesenchymal stem cell-conditioned media; CD, cluster of differentiation.

the LPS+CM group was significantly increased compared with that of the LPS group. Furthermore, H&E staining revealed that the trabecular distribution of the femur was denser in the LPS+CM group compared with that in the LPS group (Fig. 2D). These *in vivo* results indicate that AMSC-CM administration could effectively inhibit LPS-induced bone resorption.

*AMSC-CM reduces the serum levels of TNF- $\alpha$ , IL-1 and IL-6.* Since inflammation-associated cytokines are important factors that affect bone metabolism, the serum levels of TNF- $\alpha$ , IL-1, IL-6 and IL-10 were determined by ELISA in each treatment group (Fig. 3). The levels of proinflammatory cytokines (TNF- $\alpha$ , IL-1 and IL-6) and the anti-inflammatory cytokine IL-10 in the serum were significantly increased compared with the control group following stimulation by LPS. AMSC-CM treatment significantly decreased the serum levels of TNF- $\alpha$ , IL-1 and IL-6 compared with the LPS group, but had no significant effect on the level of IL-10. These results suggest that AMSC-CM reduces the production of proinflammatory cytokines during the inflammatory process, thus suppressing bone resorption.

*AMSC-CM downregulates the mRNA expression of TNF- $\alpha$ , IL-1 and IL-6.* The effects of AMSC-CM on the expression of inflammation-associated genes in RAW264.7 macrophages

following LPS treatment were investigated via RT-qPCR analysis (Fig. 4). After the macrophages were treated with LPS (1  $\mu$ g/ml) for 24 h, the mRNA expression levels of proinflammatory cytokines (TNF- $\alpha$ , IL-1 and IL-6) and the anti-inflammatory cytokine IL-10 were significantly elevated compared with those in the control group. However, the macrophages incubated with LPS+CM (5, 10 or 20  $\mu$ l/ml) exhibited a significant dose-dependent reduction in the expression of TNF- $\alpha$ , IL-1 and IL-6 compared with the LPS group. Notably, the mRNA expression levels of the anti-inflammatory cytokine IL-10 in the CM-treated groups were significantly higher compared with those in the LPS group. These results indicate that AMSC-CM beneficially modulates the response of the macrophages to LPS through elevating the expression of the anti-inflammatory cytokine IL-10 and decreasing the expression of proinflammatory cytokines.

## Discussion

Although MSC transplantation has a significant suppressive effect on the inflammatory response, there remain problems in the clinical use of MSCs, including invasive cell collection procedures, tumorigenicity and a long waiting time (11-14). Thus, numerous studies have been performed to investigate

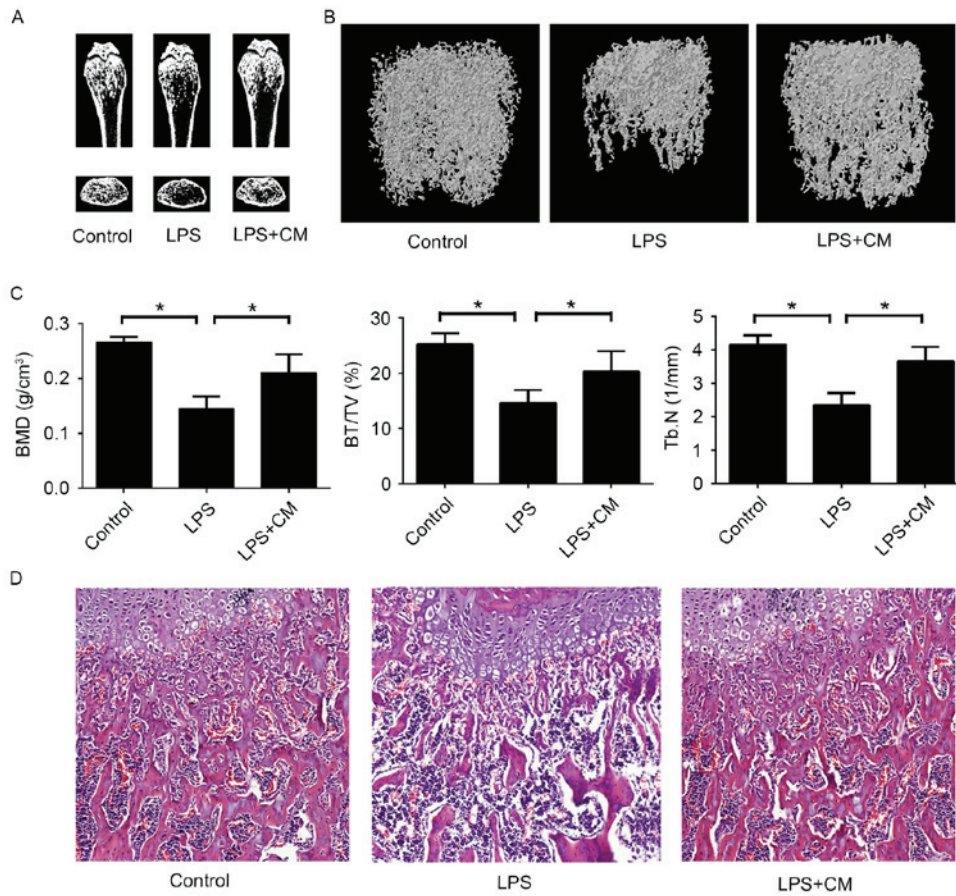


Figure 2. Adipose-derived mesenchymal stem cell-CM inhibits LPS-induced bone destruction *in vivo*. (A) Micro-CT images of the coronal and transaxial planes of the distal femurs. (B) Three-dimensional reconstructed images of the trabecular bone in the distal femurs. (C) Quantitative micro-CT analysis of the BMD, BV/TV and Tb.N of the distal femurs. \*P<0.05 as indicated. (D) Sections of the dissected femurs were stained with hematoxylin and eosin. Magnification, x100. LPS, lipopolysaccharide; CM, conditioned media; CT, computed tomography; BMD, bone mineral density; BV/TV, bone volume per tissue volume; Tb.N, trabecular number.

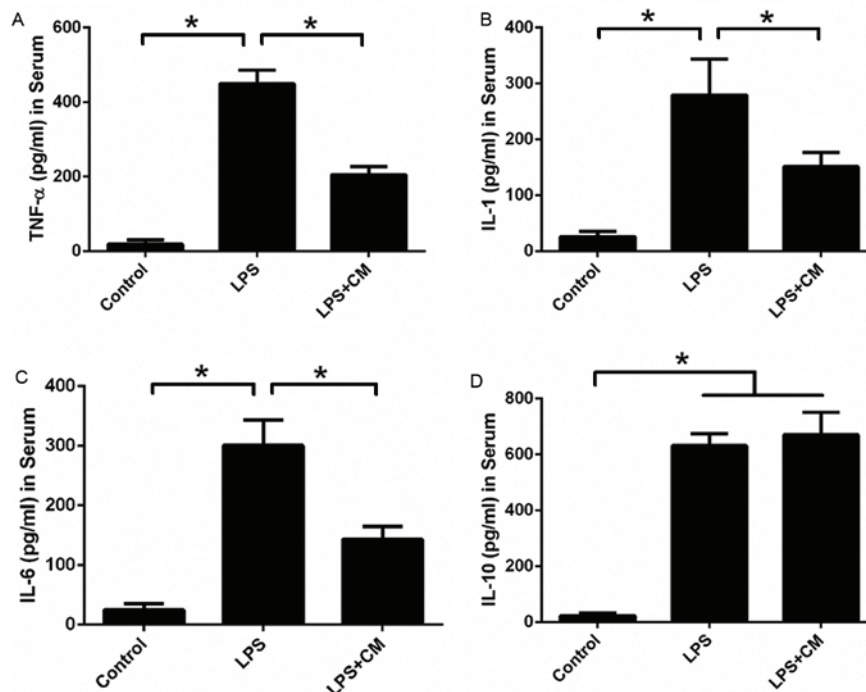


Figure 3. AMSC-CM reduces serum levels of TNF- $\alpha$ , IL-1 and IL-6. Effects of AMSC-CM on the serum levels of (A) TNF- $\alpha$ , (B) IL-1, (C) IL-6 and (D) IL-10 in mice with LPS-induced bone destruction. \*P<0.05 as indicated. TNF, tumor necrosis factor; IL, interleukin; CM, conditioned media; AMSC-CM, adipose-derived mesenchymal stem cell-CM; LPS, lipopolysaccharide.

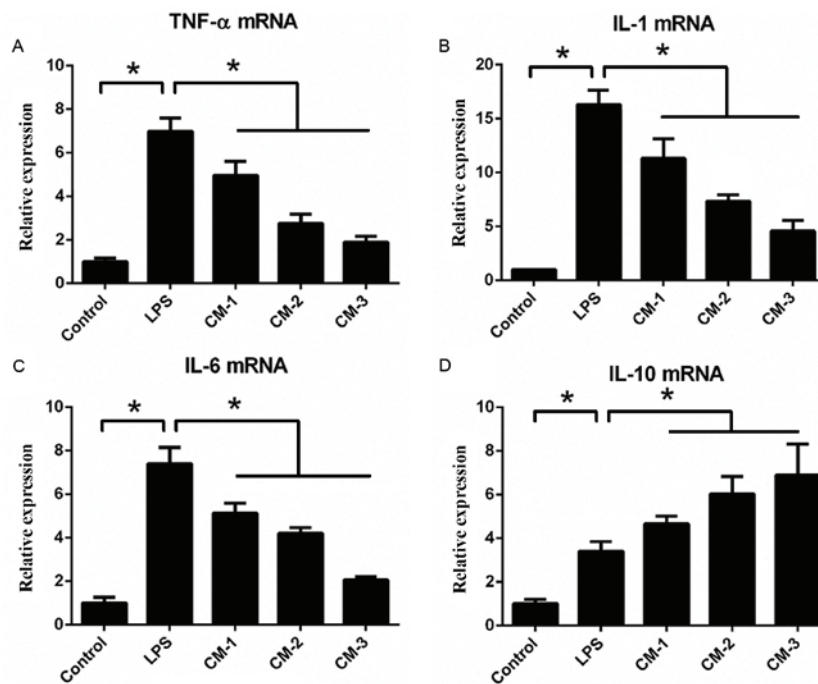


Figure 4. AMSC-CM reduces the mRNA expression of TNF- $\alpha$ , IL-1 and IL-6. Effects of AMSC-CM on the expression levels of (A) TNF- $\alpha$ , (B) IL-1, (C) IL-6 and (D) IL-10 in RAW264.7 macrophages treated with LPS. \* $P < 0.05$  as indicated. TNF, tumor necrosis factor; IL, interleukin; CM, conditioned media; AMSC-CM, adipose-derived mesenchymal stem cell-CM; LPS, lipopolysaccharide.

the effect and underlying mechanism of MSC-CM on inflammation-associated diseases (19-22). It has been reported that the factors secreted from MSCs contain inflammatory regulation factors, including transforming growth factor (TGF)- $\beta$  (TGF- $\beta$ ), TNF-stimulated gene-6 (TSG-6), prostaglandin E2 (PGE2) and hepatocyte growth factor (HGF) (24-27). TGF- $\beta$  has long been regarded as a key regulator of immunological homeostasis and inflammatory responses; it can inhibit T-cell proliferation, as well as blocking the differentiation of naive T cells into helper T cells (28). TSG-6 is a multipotent anti-inflammatory glycoprotein, which can counteract the proinflammatory effects of TNF- $\alpha$  and IL-1 (17). PGE2, a product of arachidonic acid metabolism, has been demonstrated to promote an anti-inflammatory phenotype in macrophages and increase the production of the anti-inflammatory cytokine IL-10 (29). HGF is a pleiotropic cytokine that can suppress inflammatory responses by influencing multiple pathophysiological processes, including cytokine production, antigen presentation and T cell effector function (30). However, to the best of our knowledge, the effect of MSC-CM on inflammatory bone loss has not yet been reported. The results of the present study indicate that the administration of AMSC-CM attenuates LPS-mediated inflammatory bone loss.

LPS, a component of the cell walls of gram-negative bacteria, is a typical cause of inflammation (31). The binding of LPS to its cognate receptor complex (Toll-like receptor 4, lymphocyte antigen 96 and CD14) can activate intracellular signaling pathways, including those of nuclear factor (NF)- $\kappa$ B and activator protein-1, and stimulate the production of various proinflammatory cytokines (32,33). The proinflammatory cytokines subsequently trigger the differentiation and activation of osteoclast precursors. Previous *in vivo* studies have revealed that LPS injection can induce bone loss in

short time period (33-35). Thus, an LPS-induced bone loss model is an appropriate experimental method to study the pathophysiological process of inflammation-mediated osteoporosis. As identified by the micro-CT analysis performed in the present study, the intraperitoneal injection of LPS led to significant reductions in the BMD, BV/TV and Tb.N of the distal femurs, whereas the administration of AMSC-CM effectively inhibited LPS-mediated bone resorption. Histological analysis also revealed that the LPS-induced bone destruction was suppressed by AMSC-CM. These *in vivo* results suggest that AMSC-CM protects against LPS-mediated bone loss.

During the course of the inflammatory response, a number of cytokines are activated, including TNF- $\alpha$ , IL-1, IL-6 and IL-10. Numerous cytokines serve important roles in regulating the proliferation and differentiation of osteoblasts and osteoclasts, and are therefore regarded as the mediators of inflammation-associated bone loss (5,36). TNF- $\alpha$  is a key proinflammatory cytokine during the pathogenesis of inflammation-induced bone loss; it can affect osteoclast number and activity by directly stimulating osteoclast differentiation, in addition to promoting the production of receptor activator of NF- $\kappa$ B ligand in lymphocytes and bone marrow osteoclast precursors (37). IL-1 is also a potent proinflammatory cytokine that can promote osteoclast activity, inhibit osteoclast apoptosis, and depress the proliferation and differentiation of osteoblasts (38). IL-6 is a multifunctional inflammatory cytokine, which has been reported to serve a positive regulatory role in the process of osteoclast differentiation (39). Previous studies have demonstrated that IL-6 deficient mice were protected against bone destruction in estrogen deficiency-induced osteoporosis and collagen-induced arthritis (40,41). IL-10 is a general immunosuppressive cytokine, which suppresses the activation of immune cells, decreases the production of proinflammatory

cytokines and protects the host from inflammation-induced tissue lesions (42). In the present study, the serum levels of TNF- $\alpha$ , IL-1, IL-6 and IL-10 in mice were detected to investigate the possible mechanism of the therapeutic effect of AMSC-CM on bone loss. This revealed that AMSC-CM significantly reduced the serum levels of TNF- $\alpha$ , IL-1 and IL-6 in the mice exposed to LPS, without changing the serum level of IL-10. These data suggest that AMSC-CM inhibits inflammation-induced bone loss by decreasing the production of proinflammatory cytokines.

Macrophages are important cells that mediate innate and adaptive immunity; they can regulate immune functions through phagocytizing foreign bodies, stimulating other immune cells via antigen presentation and releasing a variety of soluble factors (43). Macrophages are typically considered to be the primary source of cytokines in the process of inflammatory bone loss (44). Therefore, the effect of AMSC-CM on LPS-activated macrophages was investigated via RT-qPCR analysis. Following AMSC-CM treatment, the expression of proinflammatory cytokines was significantly inhibited in the macrophages stimulated with LPS; by contrast, there was a significantly increased expression of the anti-inflammatory cytokine IL-10. These results indicate that AMSC-CM modulates the inflammatory process through regulating the function of macrophages.

Despite the promising results, the present study also had some limitations. The RAW 264.7 cells were isolated from tumor tissue induced by the Abelson murine leukemia virus. Their response to AMSC-CM may be slightly different from that of normal macrophages. In addition, the effects of AMSC-CM on other cells associated with bone metabolism, including osteoclasts and osteoblasts, are still unclear. Therefore, further detailed study is required to clarify the biological mechanism underlying the beneficial effect of AMSC-CM on inflammation-induced bone loss.

In conclusion, the results of the current study demonstrated that the systemic administration of AMSC-CM significantly attenuated LPS-induced bone loss by reducing serum levels of proinflammatory cytokines. This beneficial effect of AMSC-CM may partly be mediated by regulating the function of macrophages during inflammatory processes. These findings indicate that AMSC-CM, as an alternative to stem cell therapy, has the potential to replace traditional treatment methods for inflammatory bone loss.

### Acknowledgements

The present study was supported by the National Natural Science Foundation of China (grant nos. 81371964 and 81572137).

### References

- Eriksen EF: Cellular mechanisms of bone remodeling. *Rev Endocr Metab Disord* 11: 219-227, 2010.
- Braun T and Schett G: Pathways for bone loss in inflammatory disease. *Curr Osteoporos Rep* 10: 101-108, 2012.
- Hajishengallis G: Immunomicrobial pathogenesis of periodontitis: Keystone, pathobionts, and host response. *Trends Immunol* 35: 3-11, 2014.
- Shaw AT and Gravalles EM: Mediators of inflammation and bone remodeling in rheumatic disease. *Semin Cell Dev Biol* 49: 2-10, 2016.
- Redlich K and Smolen JS: Inflammatory bone loss: Pathogenesis and therapeutic intervention. *Nat Rev Drug Discov* 11: 234-250, 2012.
- Lotfinia M, Kadivar M, Piryaei A, Pournasr B, Sardari S, Sodeifi N, Sayahpour FA and Baharvand H: Effect of secreted molecules of human embryonic stem cell-derived mesenchymal stem cells on acute hepatic failure model. *Stem Cells Dev* 25: 1898-1908, 2016.
- Jamnia A and Lepperdinger G: From tendon to nerve: An MSC for all seasons. *Can J Physiol Pharmacol* 90: 295-306, 2012.
- van den Akker F, Deddens JC, Doevendans PA and Sluijter JP: Cardiac stem cell therapy to modulate inflammation upon myocardial infarction. *Biochim Biophys Acta* 1830: 2449-2458, 2013.
- Liu X, Wang X, Li A and Jiao X: Effect of mesenchymal stem cell transplantation on brain-derived neurotrophic factor expression in rats with Tourette syndrome. *Exp Ther Med* 11: 1211-1216, 2016.
- Badner A, Vawda R, Laliberte A, Hong J, Mikhail M, Jose A, Dragas R and Fehlings M: Early intravenous delivery of human brain stromal cells modulates systemic inflammation and leads to vasoprotection in traumatic spinal cord injury. *Stem Cells Transl Med* 5: 991-1003, 2016.
- Timmers L, Lim SK, Hofer IE, Arslan F, Lai RC, van Oorschot AA, Goumans MJ, Strijder C, Sze SK, Choo A, *et al*: Human mesenchymal stem cell-conditioned medium improves cardiac function following myocardial infarction. *Stem Cell Res* 6: 206-214, 2011.
- Chimenti I, Smith RR, Li TS, Gerstenblith G, Messina E, Giacomello A and Marbán E: Relative roles of direct regeneration versus paracrine effects of human cardiosphere-derived cells transplanted into infarcted mice. *Circ Res* 106: 971-980, 2010.
- Stagg J: Mesenchymal stem cells in cancer. *Stem Cell Rev* 4: 119-124, 2008.
- Sell S: On the stem cell origin of cancer. *Am J Pathol* 176: 2584-2594, 2010.
- Maguire G: Stem cell therapy without the cells. *Commun Integr Biol* 6: e26631, 2013.
- Vizoso FJ, Eiro N, Cid S, Schneider J and Perez-Fernandez R: Mesenchymal stem cell secretome: Toward cell-free therapeutic strategies in regenerative medicine. *Int J Mol Sci* 18: pii: E1852, 2017.
- Madrigal M, Rao KS and Riordan NH: A review of therapeutic effects of mesenchymal stem cell secretions and induction of secretory modification by different culture methods. *J Transl Med* 12: 260, 2014.
- Wakayama H, Hashimoto N, Matsushita Y, Matsubara K, Yamamoto N, Hasegawa Y, Ueda M and Yamamoto A: Factors secreted from dental pulp stem cells show multifaceted benefits for treating acute lung injury in mice. *Cytotherapy* 17: 1119-1129, 2015.
- Chen YX, Zeng ZC, Sun J, Zeng HY, Huang Y and Zhang ZY: Mesenchymal stem cell-conditioned medium prevents radiation-induced liver injury by inhibiting inflammation and protecting sinusoidal endothelial cells. *J Radiat Res* 56: 700-708, 2015.
- Liu J, Han Z, Han Z and He Z: Mesenchymal stem cell-conditioned media suppresses inflammation-associated overproliferation of pulmonary artery smooth muscle cells in a rat model of pulmonary hypertension. *Exp Ther Med* 11: 467-475, 2016.
- Bermudez MA, Sendon-Lago J, Seoane S, Eiro N, Gonzalez F, Saa J, Vizoso F and Perez-Fernandez R: Anti-inflammatory effect of conditioned medium from human uterine cervical stem cells in uveitis. *Exp Eye Res* 149: 84-92, 2016.
- Osugi M, Katagiri W, Yoshimi R, Inukai T, Hibi H and Ueda M: Conditioned media from mesenchymal stem cells enhanced bone regeneration in rat calvarial bone defects. *Tissue Eng Part A* 18: 1479-1489, 2012.
- Livak KJ and Schmittgen TD: Analysis of relative gene expression data using real-time quantitative PCR and the 2(-Delta Delta C(T)) method. *Methods* 25: 402-408, 2001.
- Noh MY, Lim SM, Oh KW, Cho KA, Park J, Kim KS, Lee SJ, Kwon MS and Kim SH: Mesenchymal stem cells modulate the functional properties of microglia via TGF- $\beta$  secretion. *Stem Cells Transl Med* 5: 1538-1549, 2016.
- Liu Y, Zhang R, Yan K, Chen F, Huang W, Lv B, Sun C, Xu L, Li F and Jiang X: Mesenchymal stem cells inhibit lipopolysaccharide-induced inflammatory responses of BV2 microglial cells through TSG-6. *J Neuroinflammation* 11: 135, 2014.

26. Naderi EH, Skah S, Ugland H, Myklebost O, Sandnes DL, Torgersen ML, Josefsen D, Ruud E, Naderi S and Blomhoff HK: Bone marrow stroma-derived PGE2 protects BCP-ALL cells from DNA damage-induced p53 accumulation and cell death. *Mol Cancer* 14: 14, 2015.
27. Bai L, Lennon DP, Caplan AI, DeChant A, Hecker J, Kranso J, Zaremba A and Miller RH: Hepatocyte growth factor mediates mesenchymal stem cell-induced recovery in multiple sclerosis models. *Nat Neurosci* 15: 862-870, 2012.
28. Skeen VR, Paterson I, Paraskeva C and Williams AC: TGF- $\beta$ 1 signalling, connecting aberrant inflammation and colorectal tumorigenesis. *Curr Pharm Des* 18: 3874-3888, 2012.
29. MacKenzie KF, Clark K, Naqvi S, McGuire VA, Nöhren G, Kristariyanto Y, van den Bosch M, Mudaliar M, McCarthy PC, Pattison MJ, *et al*: PGE(2) induces macrophage IL-10 production and a regulatory-like phenotype via a protein kinase A-SIK-CRTC3 pathway. *J Immunol* 190: 565-577, 2013.
30. Molnarfi N, Benkhoucha M, Funakoshi H, Nakamura T and Lalive PH: Hepatocyte growth factor: A regulator of inflammation and autoimmunity. *Autoimmun Rev* 14: 293-303, 2015.
31. Bierhaus A, Chen J, Liliensiek B and Nawroth PP: LPS and cytokine-activated endothelium. *Semin Thromb Hemost* 26: 571-587, 2000.
32. An J, Hao D, Zhang Q, Chen B, Zhang R, Wang Y and Yang H: Natural products for treatment of bone erosive diseases: The effects and mechanisms on inhibiting osteoclastogenesis and bone resorption. *Int Immunopharmacol* 36: 118-131, 2016.
33. Kim JY, Ahn SJ, Baek JM, Yoon KH, Lee MS and Oh J: Ostericum koreanum reduces LPS-induced bone loss through inhibition of osteoclastogenesis. *Am J Chin Med* 43: 495-512, 2015.
34. Jin J, Machado ER, Yu H, Zhang X, Lu Z, Li Y, Lopes-Virella MF, Kirkwood KL and Huang Y: Simvastatin inhibits LPS-induced alveolar bone loss during metabolic syndrome. *J Dent Res* 93: 294-299, 2014.
35. Kim IS, Lee B, Yoo SJ and Hwang SJ: Whole body vibration reduces inflammatory bone loss in a lipopolysaccharide murine model. *J Dent Res* 93: 704-710, 2014.
36. Yu H, Li Q, Herbert B, Zinna R, Martin K, Junior CR and Kirkwood KL: Anti-inflammatory effect of MAPK phosphatase-1 local gene transfer in inflammatory bone loss. *Gene Ther* 18: 344-353, 2011.
37. Herman S, Krönke G and Schett G: Molecular mechanisms of inflammatory bone damage: Emerging targets for therapy. *Trends Mol Med* 14: 245-253, 2008.
38. Sin A, Tang W, Wen CY, Chung SK and Chiu KY: The emerging role of endothelin-1 in the pathogenesis of subchondral bone disturbance and osteoarthritis. *Osteoarthritis Cartilage* 23: 516-524, 2015.
39. Gorny G, Shaw A and Oursler MJ: IL-6, LIF, and TNF-alpha regulation of GM-CSF inhibition of osteoclastogenesis in vitro. *Exp Cell Res* 294: 149-158, 2004.
40. Poli V, Balena R, Fattori E, Markatos A, Yamamoto M, Tanaka H, Ciliberto G, Rodan GA and Costantini F: Interleukin-6 deficient mice are protected from bone loss caused by estrogen depletion. *EMBO J* 13: 1189-1196, 1994.
41. Alonzi T, Fattori E, Lazzaro D, Costa P, Probert L, Kollias G, De Benedetti F, Poli V and Ciliberto G: Interleukin 6 is required for the development of collagen-induced arthritis. *J Exp Med* 187: 461-468, 1998.
42. Hazlett LD, Jiang X and McClellan SA: IL-10 function, regulation, and in bacterial keratitis. *J Ocul Pharmacol Ther* 30: 373-380, 2014.
43. McNelis JC and Olefsky JM: Macrophages, immunity, and metabolic disease. *Immunity* 41: 36-48, 2014.
44. Hienz SA, Paliwal S and Ivanovski S: Mechanisms of bone resorption in periodontitis. *J Immunol Res* 2015: 615486, 2015.



This work is licensed under a Creative Commons Attribution-NonCommercial-NoDerivatives 4.0 International (CC BY-NC-ND 4.0) License.